ARTICLE

Study on Methanol Oxidation at Pt and PtRu Electrodes by Combining *in situ* Infrared Spectroscopy and Differential Electrochemical Mass Spectrometry

Qian Tao, Wei Chen, Yao Yao, Ammar Bin Yousaf, Yan-xia Chen*

Hefei National Laboratory for Physical Science at the Microscale and Department of Chemical Physics, University of Science and Technology of China, Hefei 230026, China

(Dated: Received on May 5, 2014; Accepted on May 23, 2014)

Methanol oxidation reaction (MOR) at Pt and Pt electrode surface deposited with various amounts of Ru (denoted as Pt_xRu_y, nominal coverage y is 0.17, 0.27, and 0.44 ML) in 0.1 mol/L $HClO_4$+0.5 mol/L MeOH has been studied under potentiostatic conditions by *in situ* FTIR spectroscopy in attenuated-total-reflection configuration and differential electrochemical mass spectrometry under controlled flow conditions. Results reveal that (i) CO is the only methanol-related adsorbate observed by IR spectroscopy at all the Pt and PtRu electrodes examined at potentials from 0.3 V to 0.6 V (*vs.* RHE); (ii) at $Pt_{0.56}Ru_{0.44}$, two IR bands, one from CO adsorbed at Ru islands and the other from CO_L at Pt substrate are detected, while at other electrodes, only a single band for CO_L adsorbed at Pt is observed; (iii) MOR activity decreases in the order of $Pt_{0.73}Ru_{0.27}$>$Pt_{0.56}Ru_{0.44}$>$Pt_{0.83}Ru_{0.17}$>Pt; (iv) at 0.5 V, MOR at $Pt_{0.73}Ru_{0.27}$ reaches a current efficiency of 50% for CO_2 production, the turn-over frequency from CH_3OH to CO_2 is ca. 0.1 molecule/(site·sec). Suggestions for further improving of PtRu catalysts for MOR are provided.

Key words: Differential electrochemical mass spectrometry, Electrochemical *in situ* infrared spectroscopy, Methanol oxidation, PtRu electrode, Current efficiency

I. INTRODUCTION

Due to the high energy density, direct methanol fuel cells (DMFCs) are of great potential as energy devices for portable electronics [1–8], however, the slow kinetics for methanol oxidation reaction (MOR) remains to be one of the major challenges for [1, 3–5, 9–14]. Extensive studies on MOR have been carried out in past decades, it is well confirmed that Pt is the best monometallic electrocatalyst for MOR [15–17]. From electrochemical differential mass spectrometry (DEMS) studies, it is found that methanol can be either completely oxidized to CO_2 or be oxidized partly to side-products such as HCHO, HCOOH, and CO_{ad} [9, 11, 12, 18]. By using electrochemical *in situ* FTIR spectroscopy under attenuated-total-reflection configuration (EC-ATR-FTIRS), we have provided quantitative information on the kinetics of CO_{ad} formation and CO_{ad} oxidation in MOR [19–21].

It is well confirmed that the addition of Ru to Pt electrocatalysts can accelerate the MOR kinetics, the enhancement induced by the addition of Ru depends critically on both the structure and composition of the PtRu catalysts [6]. A bifunctional mechanism and a ligand effect have been suggested to be the origin for the improvement in MOR activity [22]. Despite the great achievements mentioned above, no consensus for the optimal composition and structure for MOR catalysts has been reached so far. In order to develop more efficient MOR catalysts, further information on MOR mechanism, on the relationship of MOR activity with catalysts composition and structure are necessary.

In this work, we present results on MOR at Pt and PtRu electrodes in a flow cell by using combined EC-ATR-FTIRS and DEMS. Quantitative information on the development of both the surface absorbate (*i.e.*, CO_{ad}) and the volatile product CO_2 is obtained. Suggestions for further improving of PtRu catalysts for MOR will be provided based on present results and the information from literature.

II. EXPERIMENTS

Millipore Milli-Q water and perchloric acid (suprapure, Merck) are used to prepare 0.1 mol/L $HClO_4$, which is used as supporting electrolyte. Pt electrode with a thickness of ca. 50 nm on the flat reflecting face of a hemi-cylindrical Si prism formed by electroless deposition [23] is used as the working electrode (WE) or used as substrate for preparing the "Pt_xRu_y" WE,

*Author to whom correspondence should be addressed. E-mail: yachen@ustc.edu.cn

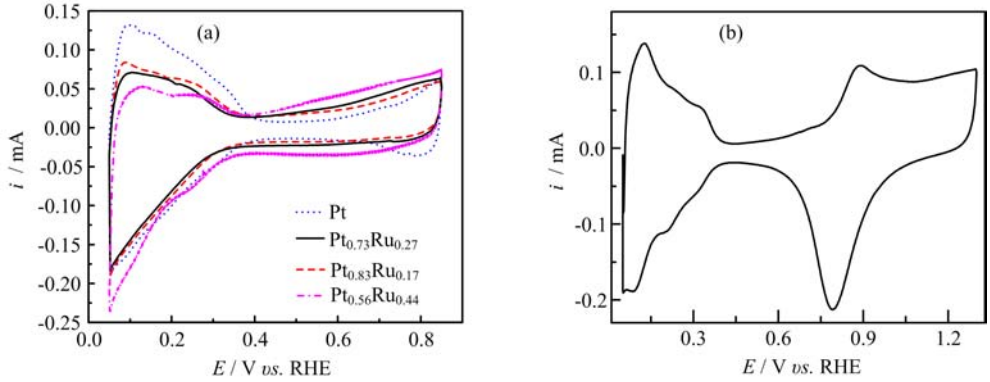

FIG. 1 (a) CV of Pt film electrode and PtRu electrodes with various nominal coverage of Ru. (b) CV of Pt film in 0.1 mol/L $HClO_4$ in the potential region from 0.05 V to 1.3 V. Scan rate: 0.02 V/s, electrolyte: 0.1 mol/L $HClO_4$.

(x and y in the subscripts of "Pt_xRu_y" represent the nominal coverage of Pt and Ru at the surface which is relative to the original active surface area of Pt electrode, x+y=1). The geometric surface area of the Pt electrode is 0.8 cm^2 and the roughness factor of the Pt electrode is ca. 7 as estimated from the charge for the oxidation of a saturated H adlayer formed in the potential region from 0.4 V to 0.05 V. A Pt gauge and a Pt wire are used as counter electrodes and a reversible hydrogen electrode (RHE) is used as a reference electrode. The dual thin-layer spectro-electrochemical flow-cell, used for EC-ATR-FTIRS, has been described in detail in Refs.[24–27], the volume of the WE compartment is ca. 15 μL, electrolyte flow rate is kept at 60 μL/s. The electrode potential is controlled using a potentiostat (CHI760 E, Shanghai ChenHua, China). All potentials quoted in this work are given versus the RHE.

Pt electrode surface is pre-cleaned by cycling in the potential region from 0.06 V to 1.3 V at a scan rate of 0.1 V/s under a continuous flow of N_2-saturated 0.5 mol/L H_2SO_4 solution, until reproducible cyclic voltammograms are obtained (shown in Fig.1(b)). Then, Ru is deposited onto the Pt electrode by flowing through a solution containing 1 mmol/L $RuNO(NO_3)_2$+0.1 mol/L $HClO_4$ for various reaction time at constant potential of 0.15 V [28]. In order to follow the kinetics for CO_{ad} formation, CO_{ad} oxidation as well as the CO_2 production, methanol oxidation reaction is examined under constant potentials from 0.3 V to 0.6 V upon switching the electrolyte solution from 0.1 mol/L $HClO_4$ to 0.1 mol/L $HClO_4$+0.5 mol/L CH_3OH, the Faradaic current, the mass spectrometric signal of m/z=44 from $^{12}CO_2$ and m/z=60 from CH_3OOCH, and the IR spectra in the range of 1000−4000 cm^{-1} are recorded simultaneously as a function of reaction time. Potentials from 0.3 V to 0.6 V are chosen for MOR, since these potentials are most relevant to what is viable in practical DMFCs.

The DEMS setup used in the present study is a HidenHPR-40 DSA Bench top-membrane inlet gas analysis system, mass signals are collected 20 points/s. The mass signal for CO_2 produced has been calibrated by oxidative stripping of a saturated CO adlayer preadsorbed at 0.06 V, mass calibration constant k=Q_F/Q_{mass} is found to be 3.65×10^6 mA/Torr in this study. The IR spectroscopic measurements are carried out using a Varian FTS-7000 spectrometer equipped with a mercury cadmium telluride (MCT) detector. A spectrum taken at the corresponding reaction potential in the supporting electrolyte is used as the reference spectrum. All spectra are obtained with a resolution of 4 cm^{-1} and 1 spectrum/s. The spectra are presented in absorbance mode, *i.e.*, $\lg(R_0/R)$, where R_0 and R are the reflectance at reference and sample potential, respectively.

III. RESULTS AND DISCUSSION

Figure 1 gives the typical cyclic voltammograms of Pt, $Pt_{0.83}Ru_{0.17}$, $Pt_{0.73}Ru_{0.27}$, and $Pt_{0.56}Ru_{0.44}$ electrodes. It is clearly seen that after the deposition of Ru, the current in H-UPD region decreases, while that in the double layer region increases. The decrease in the current for H-UPD is due to the fact that Pt sites initially for H to adsorb is now covered by Ru and the increase in the current in the double layer region is due to the oxidation of Ru to Ru-OH. The nominal coverage of Pt and Ru at the surface (relative to the original active surface area of Pt electrode) is estimated from the decrease in the charge for H-UPD. Time-resolved IR spectra in the spectral region from 1700−2200 cm^{-1} during MOR at Pt electrode after switching from 0.1 mol/L $HClO_4$ to 0.1 mol/L $HClO_4$+0.5 mol/L CH_3OH are given in Fig.2. The bands in the region of 2000−2100 and 1700−1900 cm^{-1} come from the stretching vibration of bridge- and multi-bonded CO (denoted as CO_L and CO_M) linearly. From Fig.2, it is seen that right after switching to methanol containing solution, IR bands for CO_L and CO_B appear, whose band intensity increases with time, and reaches maximum at ca. 10 s

DOI:10.1063/1674-0068/27/05/541-547

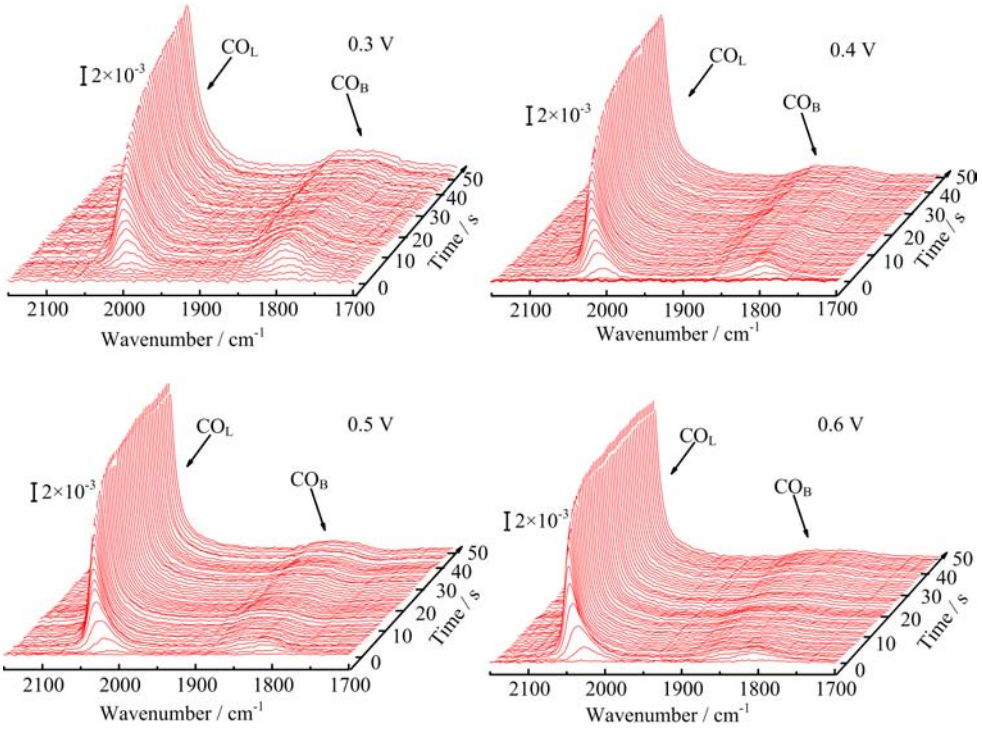

FIG. 2 Electrochemical *in situ* IR spectra recorded during the methanol oxidation on Pt electrode at 0.3, 0.4, 0.5, and 0.6 V, the electrolyte is switched to 0.1 mol/L $HClO_4$+0.5 mol/L MeOH at 0 s.

to 30 s after the solution switch. We have checked carefully the full spectral range from 1000 cm^{-1} to 4000 cm^{-1} (Fig.3), except small IR signal in the region above 3300 cm^{-1} from the stretching vibration O−H of interfacial water, no other bands from methanolic fragmentsis are observed at all the reaction potentials from 0.3 V to 0.6 V. At potentials between 0.3 and 0.5 V, the steady-state CO_L band intensity is nearly the same, which corresponds a CO_{ad} coverage of ca. 0.5 ML as estimated from a linear relationship of CO_L band intensity and CO_{ad} coverage in this coverage region [19, 20].

Time-resolved IR spectra during MOR at $Pt_{0.73}Ru_{0.27}$ and $Pt_{0.56}Ru_{0.44}$ electrodes at 0.3, 0.4, 0.5, and 0.6 V recorded upon switching the solution from 0.1 mol/L $HClO_4$ to 0.1 mol/L $HClO_4$+0.5 mol/L CH_3OH at 0 s are given in Fig.4 and Fig.5. IR spectra during MOR at $Pt_{0.83}Ru_{0.17}$ electrode are nearly the same as that at pure Pt electrode, except that the IR band intensities of CO_L and CO_M are slightly smaller (spectra are not given here). From Fig.4, it is found that CO_{ad} is also the only methanolic intermediates formed at the $Pt_{0.73}Ru_{0.27}$ electrode surface. However, compared to the case with pure Pt electrode, the IR signals for both CO_L and CO_M are much weaker, whose band intensity is ca. 10 times smaller than that at Pt electrode under otherwise identical condition. From the linear relationship between the CO_L band intensity and CO_{ad} surface coverage [19], under steady state for MOR at 0.4 V, CO_{ad} coverage at $Pt_{0.73}Ru_{0.27}$ is estimated as ca. 0.05 ML. The IR band intensity

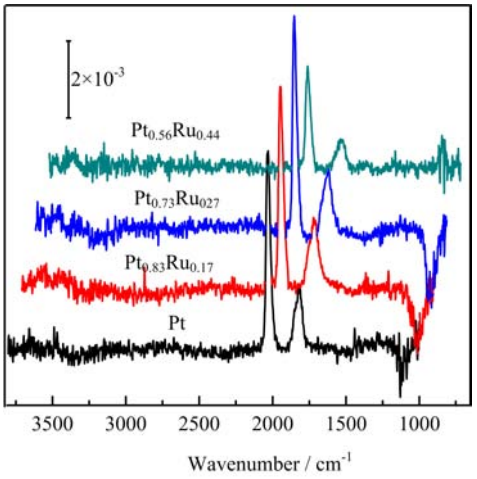

FIG. 3 Electrochemical *in situ* IR spectra recorded at 0.5 V after exposing Pt, $Pt_{0.83}Ru_{0.17}$, $Pt_{0.73}Ru_{0.27}$, and $Pt_{0.56}Ru_{0.44}$ electrode to 0.1 mol/L $HClO_4$+0.5 mol/L MeOH solution for 4 s.

for both CO_L and CO_M is found to be maximum at 0.5 V (which corresponds to ca. 0.08 ML of CO_{ad} at $Pt_{0.73}Ru_{0.27}$), it decreases toward both higher and lower potentials. The increase in CO_{ad} band intensity with potential from 0.3 V to 0.5 V is explained by the fact that at $E \leq 0.4$ V the surface is partly occupied by UPD-H atoms. As a result, the rate for methanol dehydrogenation decreases with increase in the coverage

DOI:10.1063/1674-0068/27/05/541-547

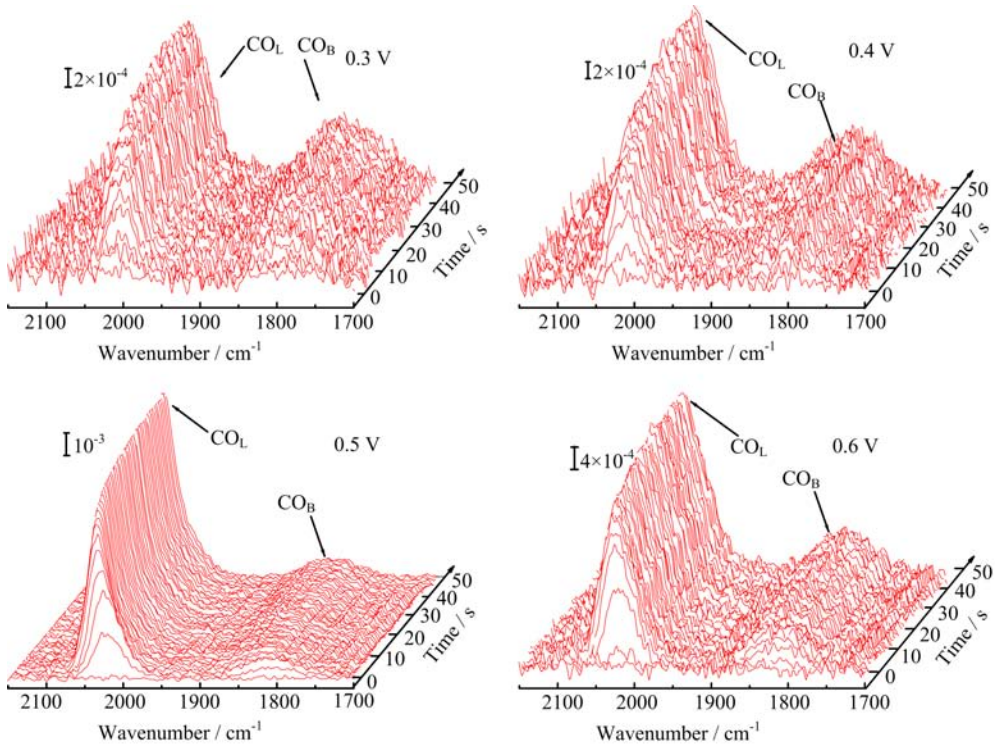

FIG. 4 Time-resolved IR spectra of CO formed during methanol oxidation on $Pt_{0.73}Ru_{0.27}$ electrode at 0.3, 0.4, 0.5, and 0.6 V, electrolyte is switched from 0.1 mol/L $HClO_4$ to 0.1 mol/L $HClO_4$+0.5 mol/L CH_3OH at 0 s.

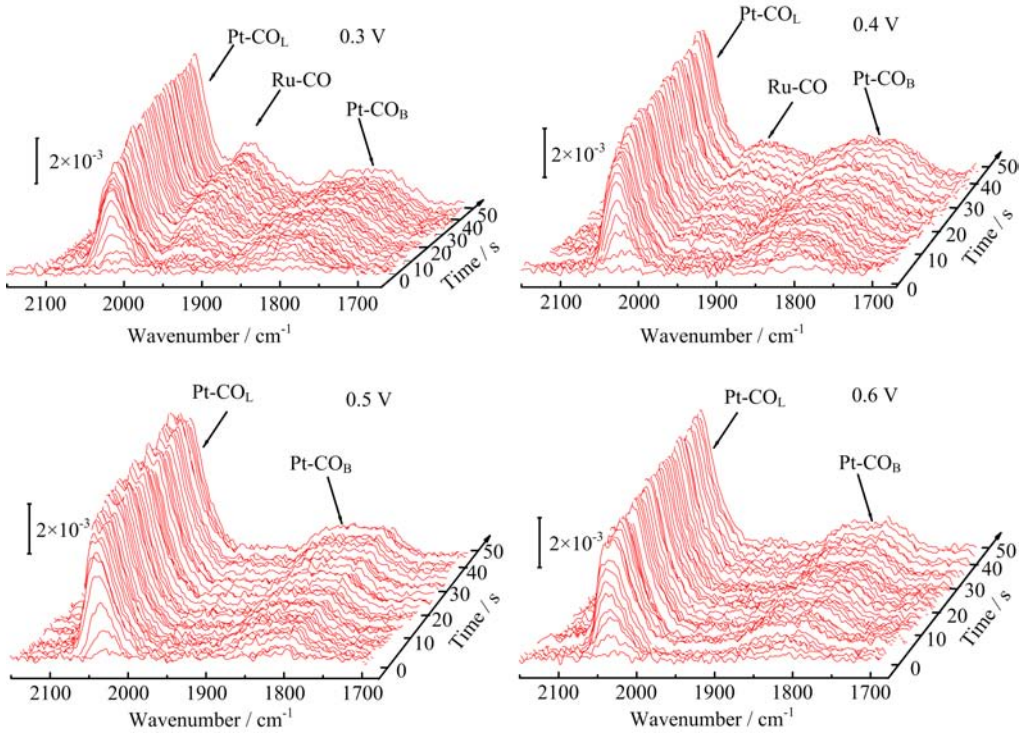

FIG. 5 Electrochemical *in situ* IR spectra recorded during the methanol oxidation on $Pt_{0.56}Ru_{0.44}$ at 0.3, 0.4, 0.5, and 0.6 V, the electrolyte was switched to 0.1 mol/L $HClO_4$+0.5 mol/L MeOH at 0 s.

DOI:10.1063/1674-0068/27/05/541-547

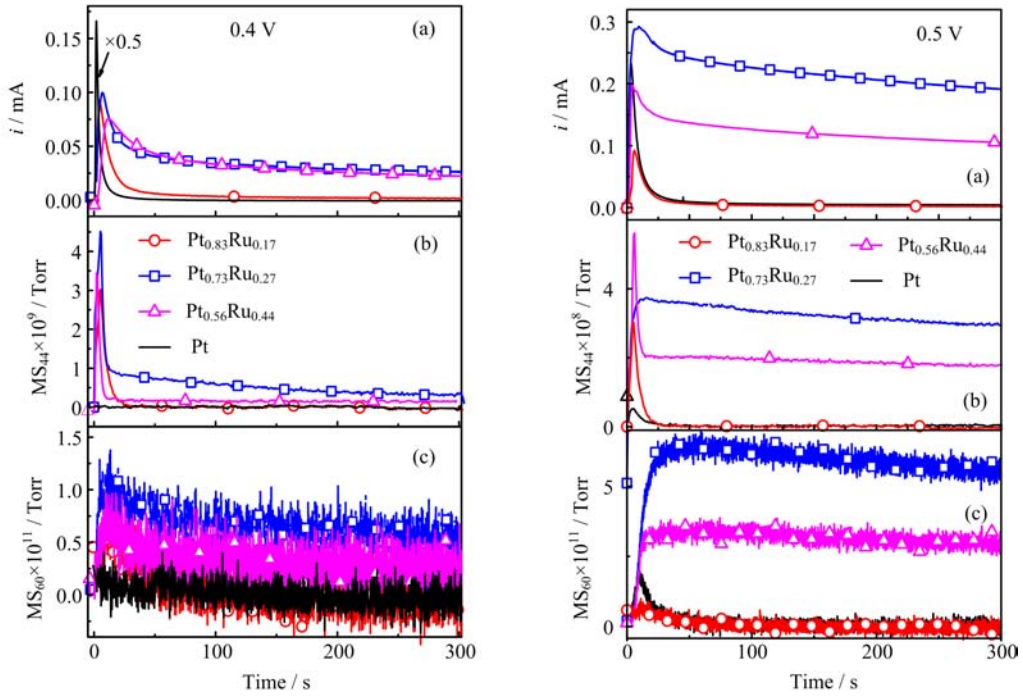

FIG. 6 Time course for (a) reaction current, mass signal of (b) m/z=44 from CO_2 and (c) m/z=60 from CH_3OOCH for methanol oxidation at Pt, $Pt_{0.83}Ru_{0.17}$, $Pt_{0.73}Ru_{0.27}$, and $Pt_{0.56}Ru_{0.44}$ electrode at 0.4 V (left) and 0.5 V (right) after solution switching from 0.1 mol/L $HClO_4$ to 0.1 mol/L $HClO_4$+0.5 mol/L CH_3OH at 0 s.

of UPD-H atoms. Results at pure Pt electrode reveal that the rate for methanol dehydrogenation increases with potential increase from 0.3 V to 0.7 V [20], the decrease in CO_{ad} band intensity at $Pt_{0.73}Ru_{0.27}$ above 0.5 V is explained by the enhanced oxidation rate of CO_{ad} by the addition of Ru.

From the IR spectra given in Fig.5 recorded during MOR on $Pt_{0.56}Ru_{0.44}$ electrode surface, it is seen that at 0.3 and 0.4 V another band in the region 1970−2020 cm^{-1} appears in addition to the IR spectra for CO_L and CO_M adsorbed at Pt as similar to the case given in Fig.4. Furthermore, it is found that the intensity of this band decreases with increase of electrode potential from 0.3 V to 0.4 V, and it disappears at higher potentials. This band is assigned to CO_L adsorbed at Ru islands, which will only appear when Ru adatoms at Pt electrodes becomes islands with large enough size (≥1 nm). Such result confirms that Ru ontop of Pt surface tends to form clusters or islands instead of epitaxial growth. These behaviors mentioned above can be explained by the faster CO_{ad} oxidation rate other than that for its formation from methanol dehydrogenation at such Ru sites.

The Faradaic currents, the mass signals of m/z=44 from CO_2 and m/z=60 from CH_3OOCH as a function of reaction time recorded during methanol oxidation on Pt, $Pt_{0.83}Ru_{0.17}$, $Pt_{0.73}Ru_{0.27}$ and $Pt_{0.56}Ru_{0.44}$ at 0.4 and 0.5 V are presented in Fig.6. When the applied potential is 0.3 V, no mass signal CO_2 and CH_3OOCH from MOR has been detected and after the initial current spike right after switching to methanol containing solution, the Faradic current drops immediately to zero (results are not shown here). From Fig.6 it is seen that immediately after switching from 0.1 mol/L $HClO_4$ to 0.1 mol/L $HClO_4$+0.5 mol/L CH_3OH at 0.4 V, MOR current at Pt film electrode increases sharply and reaches peak current at ca. 1.2 s after the solution switch. Then, it drops quickly to zero after ca. 15 s of the solution switch. At Pt electrode, no mass signal for CO_2 and $HCOOCH_3$ are detected at 0.4 V. At Pt_xRu_y, both the magnitude of the initial current spike right after the solution switch and the rate of current drop after the current spike decreases with increase in Ru coverage. MOR current on $Pt_{0.83}Ru_{0.17}$ at 0.4 V drops to zero after ca. 4 min exposing to methanol containing solution, while on $Pt_{0.56}Ru_{0.44}$, $Pt_{0.73}Ru_{0.27}$, and $Pt_{0.56}Ru_{0.44}$ electrode, a steady state current of ca. 0.03 mA can be maintained at 0.4 V.

Accompanying with the initial current spike, there are also significant mass signals for CO_2 produced from MOR on all three Pt_xRu_y electrodes at 0.4 V. After the current spike, mass signals for CO_2 drops sharply. At $Pt_{0.73}Ru_{0.27}$ a CO_2 current efficiencies of ca. 5% is attained under steady state, while at $Pt_{0.83}Ru_{0.17}$ and $Pt_{0.56}Ru_{0.44}$ the current efficiency for CO_2 production at 0.4 V are less than 1%. At all three Pt_xRu_y electrodes, the mass signal for CH_3OOCH is two orders of magnitude smaller than that for CO_2, it is not sure whether this is due to the slow kinetics for the reaction between HCOOH and CH_3OH, or just because

DOI:10.1063/1674-0068/27/05/541-547

HCOOH produced at the potential is rather small. Further studies are underway to clarify this issue. In this work, we focus on analysis of the mass signal of CO_2 together with the IR signal of CO_{ad}. The higher rate for CO_2 production on the three Pt_xRu_y electrodes at 0.4 V right in methanol containing solution, is probably due to the fact that methanol is decomposed at Pt sites neighboring to Ru to CO_{ad}, and the CO_{ad} can be oxidized easily to CO_2 with OH_{ad} previously adsorbed at neighboring Ru edges. After the consumption of OH_{ad} species at Ru, the rate for the formation of OH_{ad} at Ru sites are smaller than that for methanol dehydrogenation to CO_{ad} at Pt. Such CO_{ad} may also diffuse fast to the neighboring Ru sites. Once such sites become poisoned, the CO_2 production rate becomes very small. This is in agreement with the fact that Ru islands deposited at clean Pt catalysts surface is not good for methanol dehydrogenation, however, they are good for CO_{ad} oxidation.

At 0.5 V, at Pt and $Pt_{0.83}Ru_{0.17}$ electrodes, MOR current immediately drops to zero as similar to the case at 0.4 V. In contrast for the cases with $Pt_{0.73}Ru_{0.27}$ and $Pt_{0.56}Ru_{0.44}$, although the initial current right after switch to methanol containing solution much smaller than that for the cases at Pt and $Pt_{0.83}Ru_{0.17}$ electrodes and they are comparable to those $Pt_{0.73}Ru_{0.27}$ and $Pt_{0.56}Ru_{0.44}$ at 0.4 V, however the decay of the Faradic current with reaction time becomes much slower than the other two cases (Fig.6(a), right). Furthermore, high mass signals for CO_2 and CH_3OOCH have also been detected. The Faradic current and the mass signals from MOR at $Pt_{0.73}Ru_{0.27}$ electrode are ca. 1.5 times higher than the corresponding values at $Pt_{0.56}Ru_{0.44}$ electrode. After correcting the CO_2 mass signal with the mass calibration constant, the current efficiency for CO_2 produced from MOR on $Pt_{0.73}Ru_{0.27}$ electrode at 0.5 V is estimated to be ca. 50%, this indicates that there are still more than half of methanol molecules incompletely oxidized to HCOOH or HCHO. Additionally, both the Faradic current and the mass signals from MOR on $Pt_{0.73}Ru_{0.27}$ electrode at 0.5 V display a continuous decay. Considering that CO_{ad} coverage at Pt_xRu_y with $y\geq0.27$ is rather small (ca. 0.08 ML) and its band intensity reaches maximum at ca. 30 s after solution switch, the current decay is the most probably due to the fact that the ensemble sites for methanol dehydrogenation are not optimized.

The current density for MOR at $Pt_{0.73}Ru_{0.27}$ after normalizing to the active surface area of the Pt electrode before deposition of Ru is ca. 35 $\mu A/cm^2$ it is slightly higher than Ru deposited on Pt(111) single crystal, however it is ca. one fourth of the MOR activity reported for $Pt_{0.75}Ru_{0.25}$ alloys prepared under ultrahigh vacuum conditions through high temperature annealing [3, 29]. We have tried to use many different ways to deposit Ru onto Pt film, but we found that MOR activity at such PtRu electrocatalysts are rather small (typically <20 $\mu A/cm^2$ at 0.5 V) [30], which are similar to what has been reported typically for the PtRu system [31]. The small MOR activity are probably due to the following two factors: (i) Pt ensembles exposed at the surface are not good enough for the dehydrogenation of methanol,- (ii) Ru atoms are much less uniformly distributed in PtRu electrode in which Ru is electrochemically deposited on top of the Pt substrate than the in $Pt_{0.75}Ru_{0.25}$ alloy prepared by high temperature annealing under UHV.

The turn-over frequency (TOF) from CH_3OH to CO_2 on $Pt_{0.73}Ru_{0.27}$ is ca. 0.1 molecule/(site·sec), this number is still one order of magnitude smaller than what is required for the operation of practical DMFCs. Further optimization of PtRu nanocatalysts with ensemble structure good for methanol adsorption and its subsequent dehydrogenation, together with active Ru adatoms in its neighborhood which could accelerate oxidation of CO_{ad} and other methanolic-fragments formed at the Pt sites are necessary in order to further enhance the MOR activity. On the other hand, as mentioned above, we do not observe appreciable steady state MOR current at potentials lower than 0.3 V, which is similar to what was found for the PtRu system [32]. Further studies are underway by addition of a third element which may produce more active oxygen species for the oxidation of CO_{ad} while does not significantly inhibit methanol adsorption and dehydrogenation, in order to further reduce MOR overpotential down to 0.3 V.

IV. CONCLUSION

Methanol oxidation at Pt and Pt film electrode deposited with various amount of Ru in 0.1 mol/L $HClO_4$+0.5 mol/L MeOH has been studied under potentiostatic conditions by combining *in situ* FTIR spectroscopy and differential electrochemical mass spectrometry. We found that on all Pt and PtRu electrodes examined at potentials from 0.3 V to 0.6 V, CO is the only methanol-related adsorbate observed by IR spectroscopy. Ru deposited may only form very small clusters at Pt surface for the cases with Ru coverage below 0.3 ML, since only at $Pt_{0.56}Ru_{0.44}$, distinct IR band for CO_L adsorbed at Ru islands is detected. The overall MOR activity and CO_2 current efficiency decrease in the order of $Pt_{0.73}Ru_{0.27}$>$Pt_{0.56}Ru_{0.44}$>$Pt_{0.83}Ru_{0.17}$>Pt, the current density for MOR on $Pt_{0.73}Ru_{0.27}$ electrode at 0.5 V is ca. 35 $\mu A/cm^2$ after normalizing to the active surface area of the Pt film electrode before deposition of Ru, and the current efficiency for CO_2 production is ca. 50%, this corresponds to a turn over frequency from CH_3OH to CO_2 of ca. 0.1 molecule/(site·sec). Possible reasons for the low MOR activity of the as prepared Pt_xRu_y electrocatalysts and strategies for further improvement of MOR electrocatalysts are briefly discussed.

DOI:10.1063/1674-0068/27/05/541-547

V. ACKNOWLEDGMENTS

This work is supported by the National Natural Science Foundation of China (No.21273215), the National Instrumentation Program (No.2011YQ03012416), and the Major State Basic Research Development Program of China (No.2010CB923302).

[1] N. M. Markovic and P. N. Ross, Surf. Sci. Rep. **45**, 121 (2002).
[2] S. Wasmus and A. Kuver, J. Electroanal. Chem. **461**, 14 (1999).
[3] J. S. Spendelow, P. K. Babu, and A. Wieckowski, Curr. Opin. Solid State Mater. Sci. **9**, 37 (2005).
[4] M. T. M. Koper, S. C. S. Lai, and E. Herrero, *Mechanisms of the Oxidation of Carbon Monoxide and Small Organic Molecules at Metal Electrodes*, In: *Fuel Cell Catalysis*, Hoboken: John Wiley & Sons, Inc., 159 (2008).
[5] M. Li and R. R. Adzic, *Low-Platinum-Content Electrocatalysts for Methanol and Ethanol Electrooxidation*, In: *Electrocatalysis in Fuel Cells*, Berlin: Springer, 1 (2013).
[6] O. A. Petrii, J. Solid State Electrochem. **12**, 609 (2008).
[7] T. Iwasita, *Handbook of Fuel Cells*, Hoboken: John Wiley & Sons, Inc. (2003).
[8] C. Coutanceau, S. Brimaud, C. Lamy, J. M. Leger, L. Dubau, S. Rousseau, and F. Vigier, Electrochim. Acta **53**, 6865 (2008).
[9] A. Hamnett, *Marcel Dekker*, New York: Marcel Dekker , (1999).
[10] Y. X. Chen, A. Miki, S. Ye, H. Sakai, and M. Osawa, J. Am. Chem. Soc. **125**, 3680 (2003).
[11] T. H. M. Housmans, A. H. Wonders, and M. T. M. Koper, J. Phys. Chem. B **110**, 10021 (2006).
[12] H. S. Wang and H. Baltruschat, J. Phys. Chem. C **111**, 7038 (2007).
[13] J. L. Cohen, D. J. Volpe, and H. D. Abruna, Phys. Chem. Chem. Phys. **9**, 49 (2007).
[14] A. Miki, Y. X. Chen, S. Ye, H. Sakai, and M. Osawa, J. Am. Chem. Soc. **125**, 3680 (2003).
[15] K. Shimazu and H. Kita, Denki Kagaku **53**, 754 (1985).
[16] J. Greeley and M. Mavrikakis, J. Am. Chem. Soc. **124**, 7193 (2002).
[17] D. Cao, G. Q. Lu, A. Wieckowski, S. A. Wasileski, and M. Neurock, J. Phys. Chem. B **109**, 11622 (2005).
[18] Z. Jusys, J. Kaiser, and R. J. Behm, Langmuir **19**, 6759 (2003).
[19] L. W. Liao, S. X. Liu, Q. A. Tao, B. Geng, P. Zhang, C. M. Wang, Y. X. Chen, and S. Ye, J. Electroanal. Chem. **650**, 233 (2011).
[20] S. X. Liu, L. W. Liao, Q. Tao, Y. X. Chen, and S. Ye, Phys. Chem. Chem. Phys. **13**, 9725 (2011).
[21] B. Geng, J. Cai, S. Z. Liang, S. X. Liu, M. F. Li, and Y. X. Chen, Phys. Chem. Chem. Phys. **12**, 10888 (2010).
[22] M. Watanabe and S. Motoo, J. Electroanal. Chem. **60**, 267 (1975).
[23] Y. X. Chen, A. Miki, S. Ye, H. Sakai, and M. Osawa, J. Am. Chem. Soc. **125**, 3680 (2003).
[24] Y. X. Chen, M. Heinen, Z. Jusys, and R. J. Behm, Angew. Chem. Int. Ed. **45**, 981 (2006).
[25] Y. X. Chen, M. Heinen, Z. Jusys, and R. J. Behm, ChemPhysChem **8**, 380 (2007).
[26] M. Heinen, Y. X. Chen, Z. Jusys, and R. J. Behm, ChemPhysChem **8**, 2484 (2007).
[27] Q. Tao, Y. L. Zheng, D. C. Jiang, Y. X. Chen, Z. Jusys, and R. J. Behm, J. Phys. Chem. C **118**, 6799 (2014).
[28] C. L. Green and A. Kucernak, J. Phys. Chem. B **106**, 11446 (2002).
[29] T. Iwasita, Electrochim. Acta **47**, 3663 (2002).
[30] S. X. Liu, *Ph.D. Dissertation*, Hefei: University of Science and Technology of China, (2013).
[31] J. S. Spendelow, P. K. Babu, and A. Wieckowski, Curr. Opin. Solid State Mater. Sci. **9**, 37 (2005).
[32] A. Hamnett, *Mechanism of Methanol Electro-Oxidation*, A. Wieckowski Ed., New York: Marcel Dekker. Inc., 843 (1999).

DOI:10.1063/1674-0068/27/05/541-547